Journal of Cleaner Production 369 (2022) 133372

Contents lists available at ScienceDirect

Journal of Cleaner Production

journal homepage: www.elsevier.com/locate/jclepro

Improving air quality in Guangzhou with urban green infrastructure planning: An i-Tree Eco model study

Yibo Yao [a], Yafei Wang [a,*], Zhuobiao Ni [b,**], Shaoqing Chen [a], Beicheng Xia [a]

[a] Guangdong Provincial Key Laboratory of Environmental Pollution Control and Remediation Technology, School of Environmental Science and Engineering, Sun Yat-sen University, 135 Xingang Xi Road, 510275, Guangzhou, China

[b] Guangdong Provincial Key Laboratory of Agricultural & Rural Pollution Abatement and Environmental Safety, College of Natural Resources and Environment, South China Agricultural University, 510642, Guangzhou, China

A R T I C L E I N F O

Handling Editor: Cecilia Maria Villas Bôas de Almeida

Keywords:
Air quality
Urban green infrastructure
Local climate zone
i-Tree Eco

A B S T R A C T

With rapid economic development and increasing population, the urbanization process is accelerated, and serious air pollution threatens human health. Urban green infrastructure (UGI) planning has proven effective in improving air quality. However, how to improve air quality through UGI planning in different urban forms remains unclear. Therefore, based on the local climate zone (LCZ) of Guangzhou, this study used the i-Tree Eco model to evaluate the removal efficiency of air pollutants under different UGI designs. The results showed that from 2013 to 2019, the Built Type LCZ gradually replaced the Land Cover Type in Guangzhou, indicating the rapid urbanization process. The air pollution of the Built Type LCZs was more serious than that of the Land Cover Type. Roadside green space was more effective for air quality improvement when applied on a larger scale with the more addable area, while applying city park green space was an alternative at a local scale with limited area. The optimal designs of UGI varied within different LCZs. Adding street trees and shrubs by 20% in the urban expansion area was the optimal design for LCZ 6. For LCZ 4, adding 20% of city park trees in the urban expansion area and 5% of overall shrubs were optimal. This study proposed a practical approach for colligating the LCZ concept and i-Tree Eco simulation for air quality improvement.

1. Introduction

High intensity and rapid urbanization have significantly promoted living standards while taking up a large amount of natural resources and causing a series of environmental problems globally (Li et al., 2021; Wang et al., 2021; Wu et al., 2021; Xu et al., 2018), therefore, air pollution is an environmental problem that has attracted considerable attention. Since the severe haze event in eastern China in 2011, air pollution has frequently appeared in most northern cities and urbanized areas such as the middle and lower reaches of the Yangtze River Delta. The scope of this pollution has been spreading from north to south (Wang et al., 2020). Since the 1950s, international scholars have found that long-term exposure to air pollutants can cause cardiovascular disease, acute infectious respiratory disease, and premature death (Baetjer, 1950; Boningari and Smirniotis, 2016; Kim et al., 2015; Liang et al., 2021b). Therefore, an increasing number of researchers have conducted numerous studies focusing on the effects of urbanization on air quality and how to mitigate urban air pollution to address the gradual environmental deterioration (Aslan et al., 2021; Chu et al., 2021; Liang et al., 2019b; Tuo et al., 2013; Wang et al., 2020).

Understanding the specific drivers of urban air pollution from urbanization is a prerequisite for effectively controlling and preventing the worsening of pollution impacts. According to existing research, population aggregation and rapid economic development accompanied by urbanization will aggravate air pollution (Liang et al., 2019a; Wang et al., 2017). The urbanization process has changed land-use patterns on a large scale, both greatly and irreversibly. The concentration of air pollutants is closely related to land-use type and energy consumption structure (Lin et al., 2014). Previous research has paid more attention to the social development factors and horizontal structural changes in cities (e.g., surface features, natural elements, etc.) (Huang et al., 2021; Santri et al., 2021). However, the urban form can be altered both horizontally and vertically during urban expansion. From the perspective of three-dimensional space, the structure, height, and density of urban

* Corresponding author.
** Corresponding author.
E-mail addresses: wangyf97@mail.sysu.edu.cn (Y. Wang), nizhuobiao@scau.edu.cn (Z. Ni).

https://doi.org/10.1016/j.jclepro.2022.133372
Received 31 March 2022; Received in revised form 13 July 2022; Accepted 26 July 2022
Available online 1 August 2022

buildings and vegetation in vertical space can change the radiation reception and temperature, reduce the gas flow rate and affect pollutant dispersion (Lei et al., 2021; Liang et al., 2021a; Wang et al., 2021; Zhao et al., 2022). To comprehensively analyze the relationship between urban spatial structure and air quality changes under the process of urbanization, local climate zones (LCZs) have been widely used in recent years as a method to study urban microclimate and urban spatial structure. The LCZ method consists of two categories, built types and land cover types (Stewart and Oke, 2012). There are three classification methods of LCZ which are manual sampling, GIS, and remote sensing imaging. The first approach is time-consuming, overworked, and rarely used. The second method entails classifying the study area using the LCZ types corresponding to each urban morphological parameter range (Estacio et al., 2019; Hidalgo et al., 2019; Oliveira et al., 2020; Quan, 2019; Zheng et al., 2018). Although the accuracy of the results is high, this approach requires high data comprehensiveness and accessibility. To improve efficiency and increase the availability of LCZs on a larger scale (Cai et al., 2016), researchers mostly use high-definition remote sensing satellite images to classify and extract surface morphological indicators (Chen et al., 2021; Eldesoky et al., 2021; La et al., 2020). To support this method, the World Urban Database and Portal Tool[1] (WUDAPT) was developed to classify LCZs (Mills et al., 2015; Zhou et al., 2020). Many studies use its basic or modified methods for various applications and research (Brousse et al., 2016; Chen et al., 2020; Ching et al., 2019; Wang et al., 2018). In general, many research analyses on urban heat island and surface temperature correlations have been conducted by predecessors using LCZs (Chen et al., 2021; Holec et al., 2020; Khamchiangta and Dhakal, 2021; Yang et al., 2020, 2021). On this basis, the human thermal comfort and subjective thermal sensation of pedestrians have been studied (Lau et al., 2019). However, there have been few studies on the application of LCZs to the distribution of air pollution closely related to urban spatial structure.

Urban green infrastructure (UGI) refers to the interconnected network of green spaces, including greenways, wetlands, rainforests, forests, native vegetation, etc. (Benedict and McMahon, 2002; Foster et al., 2011). The removal of air pollutants, such as sulfur dioxide (SO_2), nitrogen oxides (NOx), carbon monoxide (CO), and particulates, is an important ecosystem service generated by UGIs (Bottalico et al., 2016; Zhang et al., 2020). However, biogenic volatile organic compounds (BVOCs) from vegetation contribute to the formation of O_3 and secondary organic aerosols, which are closely related to tree species (Calfapietra et al., 2013; Ren et al., 2017). It is particularly important to properly plan the UGI to optimize its air quality improvement. The i-Tree model is an urban forest benefit analysis and evaluation software that was released by the USDA Forest Service in 2006. i-Tree Eco is one of the software tools used to estimate the value of ecosystem services provided by vegetation based on its parameters, and it uses the dry deposition method of the previous UFORE model to calculate the removal of pollutants by various types of plants during non-precipitation periods (Jayasooriya et al., 2017; Riondato et al., 2020; Selmi et al., 2016). The model can be directly used in the United States, Europe, and Australia, and contains more than 95% of the basic urban information and corresponding species data. However, the application of the i-Tree Eco model in China is still in its infancy, and there is a lack of comprehensive evaluation of the removal of air pollutants by UGI and related economic benefits. Thus, little is known about the impact of the planning and design of different properties and element combinations of UGI on air pollution removal.

To this end, we attempted to develop a practical approach based on the integration of LCZ designs and i-Tree Eco to seek the most effective UGI strategies for ameliorating the air pollution problem. Hence, this study applied the LCZ scheme to analyze the urbanization and concentration distribution of air pollutants in Guangzhou. Based on the pollutant concentrations in different LCZs, the i-Tree Eco model was used to quantify the air pollution removal by UGI in different LCZ types. Subsequently, the UGI type and area in each LCZ were changed in the i-Tree Eco model to explore optimal UGI planning. The purpose of this study was to provide decision-makers and urban planners with information on the variation in air pollutant distribution with different urban forms and greening and to provide suggestions for UGI planning and construction.

[1] https://www.wudapt.org/.

2. Materials and methods

2.1. Study area

Guangzhou (112°57′-114°3′E, 22°26′-23°56′N) is the capital of Guangdong Province. It is the core engine and focal point of the development of the Guangdong-Hong Kong-Macao Greater Bay Area. The topography is high in the northeast and low in the southwest. It has a maritime subtropical monsoon climate with no apparent seasonal changes. The annual average temperature is 21.9 °C, and the annual precipitation is approximately 1736 mm. Guangzhou covers an area of 7434.4 km^2 and has a population of 15,305,900, with a high population density. In 2019, Guangzhou's GDP was 2362.86 billion yuan, ranking second in the province and among the top four regions in the country. There are 11 districts in the city, namely, Yuexiu, Liwan, Haizhu, Tianhe, Baiyun, Huangpu, Nansha, Panyu, Huadu, Zengcheng, and Conghua, of which the first seven districts developed earlier and the last four are considered the "new four districts". The urbanization rate of Guangzhou is 86.46%, which is higher than the national level of 60.60%. In the past 40 years, the urban land area of Guangzhou has expanded 21.2 times (Meng et al., 2020). Due to state control and greenfield protection, urban air quality has had an improving trend, with an annual average $PM_{2.5}$ concentration of 30 μg/m^3 in 2019, meeting the national secondary standard. However, there was a dramatic seasonal difference; the maximum $PM_{2.5}$ concentration in winter has been recorded to be as high as 75 μg/m^3, and only 50% of the days reached the standard of air quality.

2.2. Data and methods

The research process included three steps: (1) the distribution of $PM_{2.5}$ in Guangzhou in 2019 was obtained from ArcGIS; (2) the LCZ map of Guangzhou in 2019 was drawn and the current urban spatial morphology of Guangzhou was analyzed; and (3) the i-Tree Eco model was adopted to simulate the current situation of air pollution removal by UGIs in various LCZs, and scenario analysis was conducted to explore the optimal UGI design.

2.2.1. The distribution of $PM_{2.5}$

2.2.1.1. Data source. The $PM_{2.5}$ concentration data in this study were obtained from 38 air quality monitoring stations, 12 of which are located within Guangzhou city, and the other 26 are in the five cities around Guangzhou, namely Foshan, Qingyuan, Huizhou, Dongguan, and Zhongshan (Fig. S1). Hourly concentration data from each monitoring station were downloaded from the National Real-Time Urban Air Quality Release Platform of the China General Environmental Monitoring Station (https://air.cnemc.cn:18007/). Using these data, the annual average $PM_{2.5}$ concentration from 0:00 on January 1, 2019 to 23:00 on December 31, 2019 was calculated.

2.2.1.2. Spatial interpolation. It is physically impossible to obtain the continuous pollutant concentration data of each spatial location in the study area. Spatial interpolation methods can be used in ArcGIS to estimate data for unmonitored areas by using the data from existing monitoring stations (Jiang et al., 2021). Some studies have shown that the ordinary kriging method (OKM) has higher accuracy and the best results in estimating air pollutant concentrations in areas without monitoring stations in the Pearl River Delta region (Zhang et al., 2021).

2.2.2. Local climate zone (LCZ) map

LCZ is defined as "an area of uniform surface cover, structure, material, and human activity spanning hundreds of meters or kilometers on a horizontal scale" (Stewart and Oke, 2012). It was first proposed by Auer, an American meteorologist in 1978 (Auer, 1978; Ellefsen, 1991) and was later modified by (Stewart and Oke, 2012) into a more concise system of climate zones. The LCZ method is globally transferable and can be modeled and studied worldwide (Demuzere et al., 2019), including ten Built Types (LCZ 1–10) and seven Land Cover Types (LCZ A-G) (Stewart and Oke, 2012). The surface characteristics and definitions of each subcategory are described in Fig. S2. The classification requires detailed data on urban morphology; however, these data are difficult to obtain due to technical and policy constraints in the study area. The WUDAPT was developed to capture information on urban form and function based on the principle of generating "fit-for-purpose" urban data using a globally consistent methodology and publicly accessible input data and tools. The products are shared across multiple communities and platforms (Ching et al., 2018). It mainly contains three levels, among which the WUDAPT level 0 classification method is generally used for city and climate modeling at mesoscale and is suitable for determining LCZ classification at the city level (Wang et al., 2018). The main processes include downloading the Landsat remote sensing images, resampling the spatial resolution from 30 to 100 m to improve the accuracy of their automatic classification, digitizing the training samples in Google Earth as reference data, and using the classification tool in the open-source software SAGA GIS to realize LCZ partitioning. Finally, the assessment was conducted using a confusion matrix (Table S1). The detailed steps applied for the LCZ classification are presented in the Supporting Information (Text S1).

2.2.3. I-Tree Eco model

The air pollution removal by UGI in Guangzhou city was estimated using the i-Tree Eco model. The ability of different species of trees or shrubs to remove five air pollutants ($PM_{2.5}$, NO_2, CO, SO_2, and O_3) has been differentiated and evaluated within the latest version of the model (V6). The model requires tree properties (incl. tree species, height, diameter at breast height (DBH), canopy width and cover, etc.) and shrub properties (incl. species, shrub group height, degree of dieback, percentage of each type, etc.). A large number of studies have analyzed the improvement of UGI on air quality by i-Tree Eco model and the accuracy of the model was widely accepted (Jayasooriya et al., 2017; Nowak et al., 2016; Riondato et al., 2020; Wu et al., 2019). Combined with local meteorological data and pollution data, the amount of air pollutants removed by trees and shrubs was estimated using the method set up in the model.

2.2.3.1. Data collection. The i-Tree model has a separate database (i-Tree Database) that contains the geography of some cities around the world and their corresponding meteorological and air pollution data for certain years. However, the application of this model in China is still in its infancy, and the information for Guangzhou city is not in the database. Thus, it was necessary to input the geographic, meteorological, and air pollutant data of the investigated year into the i-Tree Database. The administrative level, latitude, longitude, elevation, average minimum temperature, population, area, etc., were obtained from the Guangdong Province Statistical Yearbook 2019. The hourly precipitation data were collected from the National Climatic Data Center (NCDC) weather station in Baiyun District, Guangzhou. The China General Environmental Monitoring Station shows that there are 12 air pollutant monitoring stations in Guangzhou city. According to the method summary of the i-Tree Eco model,[2] the average value of the data of all monitoring points should be taken as the final pollutant data. Therefore, the hourly concentration values of $PM_{2.5}$, PM_{10}, NO_2, CO, SO_2, and O_3 of the 12 air pollutant monitoring stations in Guangzhou were collected from the national urban air quality real-time publishing platform. Subsequently, the annual concentration data of six pollutants in 2019 were calculated.

2.2.3.2. Field sampling. The constant updating of the i-Tree Eco model makes it possible to determine different sampling methods based on the characteristics of the study area. Our study area covered the whole city of Guangzhou, and it was impossible to statistically assess all vegetation. The partial sampling method requires random sampling sites, which consist of two options: stratification or non-stratification. An unstratified approach directly selects random sampling plots in the study area, and this approach is simple to operate but will deviate from the study objectives. For stratified sampling, the study area is divided into strata or smaller units, and plots are randomly selected in each stratum. The number of plots depends on the level of interest of the researcher, plot variability, or stratigraphic coverage (i-Tree Eco Users' Manual, 2020). Based on the research objectives of this study, the stratified sampling method was selected, and the model was constructed using LCZ type as stratification.

After determining the appropriate sampling method, it was necessary to determine the number and size of random sampling plots in each stratum. The accuracy of the model and the time and cost of field data acquisition should be considered comprehensively. To determine the information of sampling plots suitable for various research areas, Nowak et al. (2008) found that the decreasing speed of model error decreased with the increase in sampling plots. Balancing efficiency and labor costs, the optimal number of plots for an urban area was 200 at least, with a minimum of 20 sampling plots per stratum and an area of 0.04 ha (20 × 20 m) per plot. In this study, each LCZ type was taken as a stratum and the sample numbers of each stratum are shown in Table S2. The number of plots in each stratum was determined according to the area and pollution level of each LCZ in Guangzhou. According to the results and attributes of LCZs, there were no sampling points in LCZ 7 (non-existent), LCZ 9 (too small), and LCZ F (no vegetation). Random samples of each stratum were created and the locations of random sampling plots were determined using Google Earth and ArcGIS software according to the steps of selecting stratified random sampling points in the i-Tree Eco Field Guide. The distribution of sampling points is shown in Fig. S3.

Field survey sampling was conducted during a warm period in 2020. According to the requirements for data collection in the i-Tree Eco User's Manual, the sampling point was a circular area with an area of 0.04 ha. To facilitate field operation, sampling data, including plot information and complete tree and shrub data, were collected within a 20 × 20 m plot, as shown in Table S3. Pictures of field sampling are shown in Fig. S4.

2.2.3.3. Simulation settings. Based on meteorological and pollutant data and vegetation information submitted from field surveys, i-Tree Eco quantifies the contribution of common UGI to air quality improvement. The detailed model setting is shown in Fig. 1. First, the project type of this study was selected based on the sampling type. Second, Guangzhou was stratified and the number of sampling points in each stratum was determined according to LCZ distribution. Third, the detailed vegetation data from the field sampling were manually filled into the model. Finally, the simulation results were reported after running the model.

[2] https://www.itreetools.org/documents/650/Understanding_i-Tree.gtr_nrs200.pdf.

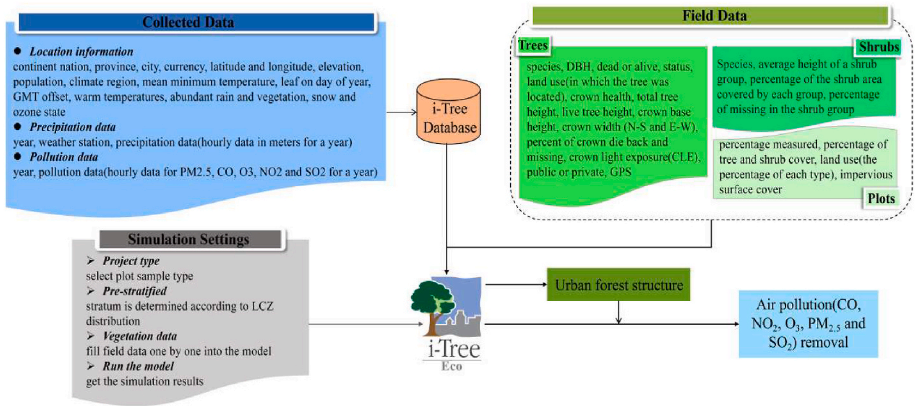

Fig. 1. The main procedure for operating the i-Tree Eco (according to i-Tree Eco manual).

2.2.4. UGI scenarios

To explore the optimal UGI design for Guangzhou, this study compared and analyzed the removal of air pollutants by adding different types and amounts of vegetation. The UGI scenarios were as follows:

2.2.4.1. Adding trees. Two tree species were selected to represent two UGI types, one is *Ficus microcarpa* representing roadside green space/trees and another is *Mangifera indica* representing city park green space/trees. There were two designs for adding trees: first, two types of trees with 5% and 10% of the vegetation coverage area (canopy area) were respectively added in each Built Types of LCZs and LCZ E, which were greatly affected by traffic. Second, two types of trees were added only in urbanized areas during 2013–2019 to alleviate the deterioration of air quality caused by urbanization. The number of integer samples that need to be changed was determined according to the proportion of urban expansion areas in each LCZ type. For the extra decimal portion (i.e., the portion less than one sample), the area that needs to be changed for an individual sample was calculated. Afterwards, two different tree species with 5%, 10%, and 20% of the vegetation coverage area were added to the samples that were determined to change (Table 1).

2.2.4.2. Add shrubs. As a major vegetation type for the UGIs including green walls and green roofs, one representative shrub species (i.e., *Loropetalum chinense*) was added to explore its effects on air quality. To ensure comparability, the methods and proportions of adding were consistent with the tree scenarios. The details of the scenarios of adding trees and shrubs are shown in Table 2.

Table 1
The number and area of samples to be changed.

LCZ	Number of samples	Proportion of area from Land Cover to Built Types	Number of samples to change	Area of change except integer samples number (m^2)
1: Compact high-rise	20	12.32%	2	188.20
2: Compact mid-rise	10	17.35%	1	297.69
3: Compact low-rise	2	7.72%	0	62.50
4: Open high-rise	5	23.64%	1	73.79
5: Open mid-rise	12	35.46%	4	103.15
6: Open low-rise	2	47.77%	0	386.91
8: Large low-rise	2	31.14%	0	252.21
10: Heavy industry	10	10.31%	1	12.73
E: Rock paved	5	42.02%	2	40.80

3. Results and discussion

3.1. Local climate zone in Guangzhou from 2013 to 2019

According to the WUDAPT method, Fig. 2 shows the LCZ map of Guangzhou in both 2013 and 2019 as well as the changes in each district. From an overall perspective, LCZ A covered the largest area in Guangzhou and was concentrated in the north. In the south, the water area covered a wide range, while the central part was a highly developed urban area with a large built-up area and high density. The LCZ changes from 2013 to 2019 were mainly dominated by the growth of open buildings (LCZ 4–6), of which LCZ 6 was 3.5 times larger in 2019 than that in 2013. The architectural composition gradually changed to the high-density type dominated by office buildings and the low-density type dominated by villas for comfortable living. Due to the increase in Guangzhou's population, LCZ 3 increased by nearly three times, and LCZ 1 increased by 17.45%. Meanwhile, the industry developed rapidly, with an area increase of 21.82%. The built-up area of Guangzhou city increased by 5% in 6 years. Although the area of LCZ A-C increased slightly due to the construction of parks, residential areas, and campuses within the city to increase the green coverage, the natural coverage area still decreased. This finding was generally in line with other studies in Guangzhou. Xie and Liu (2019) and Zhuang (2019) reported that the urban green coverage rate in Guangzhou has had a downward trend. With the increase in urban buildings, urban green spaces presented a fragmented and regular development trend. Furthermore, Fig. 2 shows that the cities are expanding continuously, and the LCZ 4 represented by the agricultural land was reduced by 60%. This finding was in line with a previous study reporting that the reduction in agricultural land was the most remarkable among the changes in urban spatial patterns in Guangzhou, mainly because of the effect of urban expansion on suburban agricultural space (Zhang and Yang, 2021). The water area was reduced by 21%, mainly due to the reclamation project (Wang et al., 2021).

From the perspective of each district, the built-up areas of Zengcheng and Conghua Districts with a large amount of vegetation coverage increased in a wide and large range. LCZ 6 of Zengcheng and LCZ 5 of Conghua in 2019 were 5 and 8 times higher than those in 2013, respectively. LCZ E in Conghua District increased by 7.6 times with rapid traffic development, representing the largest increase among all districts. Huadu, Baiyun, and Huangpu Districts in the north-central part of the city had a combination of natural and urbanized areas. The built-up area in these districts obviously expanded. LCZ 3 of Huadu in 2019 was 16 times higher than that in 2013, while LCZ 6 was 6.6 times higher. LCZ E also increased, indicating that transportation in this area was

Table 2
The details of the scenarios of adding trees and shrubs.

Scenarios						
Types of UGI		Increase 5% green cover in whole built-up area	Increase 10% green cover in whole built-up area	Increase 5% green cover in urban expansion area	Increase 10% green cover in urban expansion area	Increase 20% green cover in urban expansion area
Tree	Street Trees	T_1	T_2	T_3	T_4	T_5
	Fruit Trees	T_a	T_b	T_c	T_d	T_e
Shrub		S_1	S_2	S_3	S_4	S_5

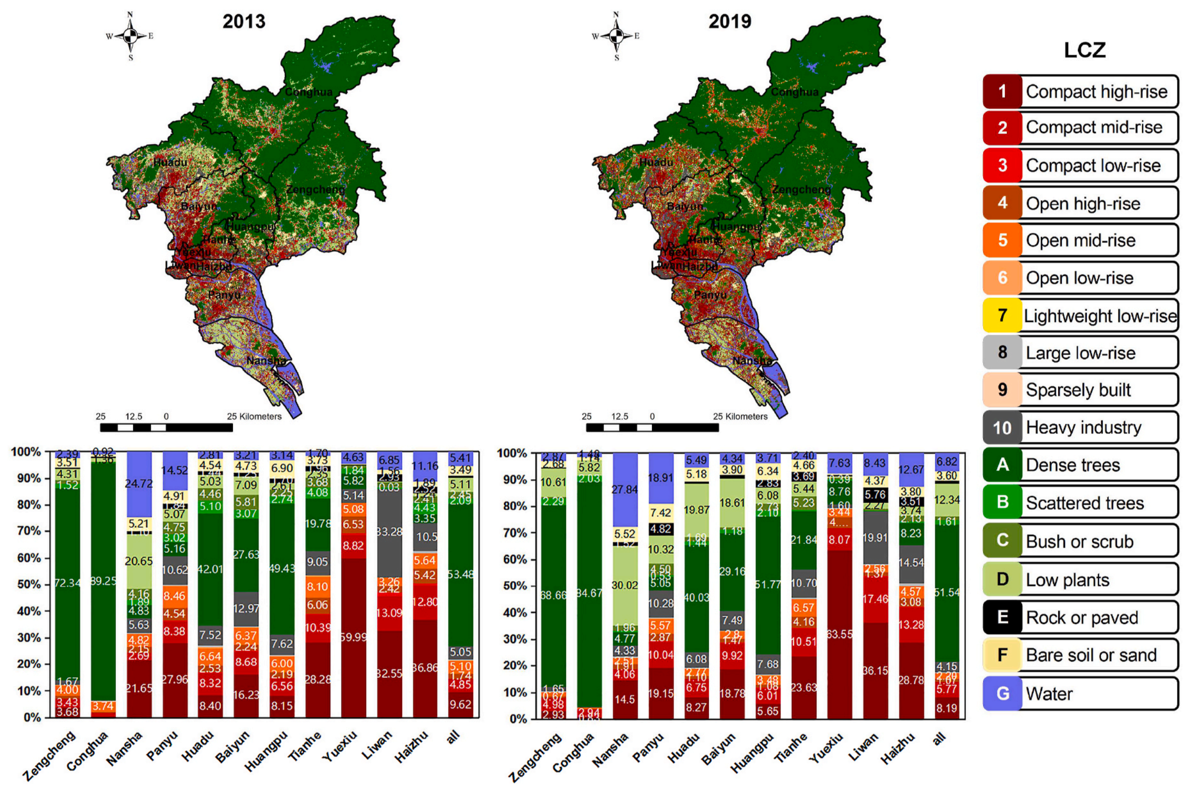

Fig. 2. Local climate zone in Guangzhou from 2013 to 2019.

continuously convenient and that regional development was accelerating. The open buildings (LCZs 4–6) and industry area (LCZ 10) in Baiyun District had prominent growth. Fan (2019) reported that the reason for this growth was closely related to the geographical location of Baiyun District, which belongs to the suburban countryside and has absorbed a large number of people. With the increase in rural housing, a large number of small workshops and a heavily polluted chemical industry appeared. As an early industrial area, Huangpu District had been optimizing its industrial structure, slowed its polluting industries, and built dense high-rise buildings to create a prosperous regional image. Its LCZ 1 increased by 45% between 2013 and 2019. The Yuexiu, Liwan, Tianhe, and Haizhu Districts in the center of Guangzhou are highly urbanized areas. A large local population lives in Yuexiu and Liwan, leading to the fact that most of the buildings in the two districts are residential buildings. Due to their development being close to the saturated level, the variability was limited, and the influx of the foreign population continued (Huang, 2017). The "urban villages" dominated by LCZ 3 in the two districts have increased by 11 and 3 times, while LCZ A has decreased by 34% and 33%, respectively, in six years. A large area of green space has been reduced to meet people's living needs. Tianhe and Haizhu Districts were characterized by dense buildings (LCZ 1–3), accounting for approximately 45% in 2013, and the proportion increased to 48% in 2019. LCZ B in the two districts increased by 7 and 11 times, respectively. In general, LCZ D and LCZ G in all 11 districts decreased, indicating that Guangzhou's urban expansion was accelerating and moving toward an economic trend of high quality and structural excellence to some extent.

3.2. Relationship between $PM_{2.5}$ and LCZ

Fig. 3 shows the differences in the $PM_{2.5}$ concentration of each LCZ. Except for the apparently low $PM_{2.5}$ concentration of LCZ 9, the differences between the other LCZ types were not obvious. The overall $PM_{2.5}$ concentration ranged from 26 to 33 μg/m^3, meeting the target of 35 μg/m^3 set by the World Health Organization (WHO) in the first transitional period. However, this value is still far from the standard value of 10 μg/m^3. The mean $PM_{2.5}$ value of the built type (LCZ 1–10, LCZ E) was 29.82 μg/m^3, which was approximately 2.7 μg/m^3 higher than that of the land cover type (LCZ A-G except for LCZ E).

Among the other built-up types, LCZ 3 had the largest mean concentration of $PM_{2.5}$. The main reason was the concentrated population, complicated traffic, and large $PM_{2.5}$ emissions in LCZ 3. Furthermore, the impermeable surface and high-density buildings create poor diffusion conditions. LCZ 10 had the second-largest mean concentration of $PM_{2.5}$. This LCZ type was a heavy industrial area with high air pollutant emissions and a large number of transport vehicles accessing the factory;

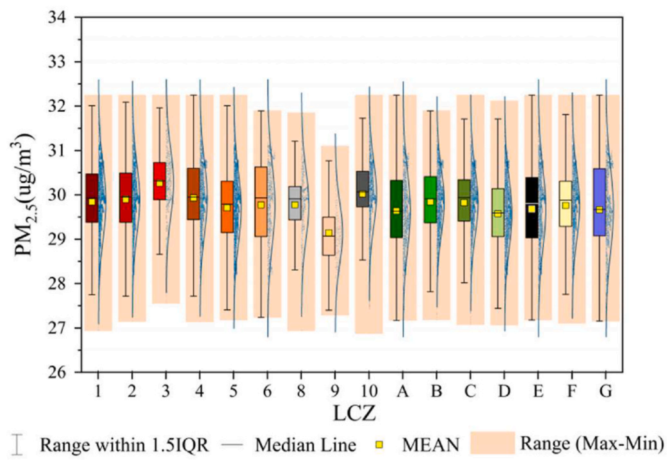

Fig. 3. The concentration of $PM_{2.5}$ in LCZs in Guangzhou (the box plots show the distribution of $PM_{2.5}$ for each LCZ; the pink squares show the range of $PM_{2.5}$ for each LCZ).

hence, the $PM_{2.5}$ concentration was high. The mean $PM_{2.5}$ concentrations of LCZ 1, 2, and 4 were similar (29.93, 29.90, and 29.84 μg/m^3, respectively) and, sorted from high to low, were LCZ 4 > 2 > 1. This finding was basically consistent with previous studies on urban heat islands and wind fields, which showed that the urban heat island effect of high temperature, low air density, and low wind speed significantly contributes to the formation of $PM_{2.5}$ (Huang et al., 2021). Wang et al. (2021) reported that the urban heat island effect in Guangzhou, from high to low, was LCZ 3, 2, 4, and 1. In addition, LCZ 1 had the highest urban heat island effect at night. The higher the building height and density are, the stronger the interference and inhibition of the urban wind field, affecting the diffusion of pollutants (Shi et al., 2019; Xu et al., 2020; Yang et al., 2019). The wind speed gradually decreased from sparse and open low-rise areas to dense mid-rise areas, leading to a high concentration of $PM_{2.5}$ in high-density or high-rise built-up areas (Zhao et al., 2020).

For the land cover type, LCZ A had the lowest mean $PM_{2.5}$ concentration (29.64 μg/m^3), which was related to the good conditions for $PM_{2.5}$ adsorption and deposition provided by the dense tree coverage in LCZ A (Liu et al., 2014). Compared with LCZ A, the $PM_{2.5}$ concentrations in LCZ B and LCZ C were relatively high, at 29.84 μg/m^3 and 29.82 μg/m^3, respectively. This result may be because these two LCZ types were mainly distributed in city parks, campuses, or residential areas, which are greatly affected by human activities.

Fig. 3 shows the mean, maximum, and minimum $PM_{2.5}$ concentrations for each LCZ class. As a dense high-rise building, the range of $PM_{2.5}$ concentrations in LCZ 1 was the largest, indicating that the regional disparity was obvious. The more clustered LCZ 1 was, the higher the $PM_{2.5}$ concentration was, and vice versa. LCZ 9 had the smallest range of $PM_{2.5}$ concentrations, mainly because this LCZ type was less distributed in Guangzhou. To meet the stratification requirements of the i-Tree Eco model, LCZ 9 was no longer considered in the i-Tree Eco construction.

3.3. UGI simulation

3.3.1. Current status analysis

Before scenario analysis, it was necessary to evaluate the impact of existing green infrastructure on urban air quality. Furthermore, to determine the impact of trees and shrubs in each LCZ, simulations of tree

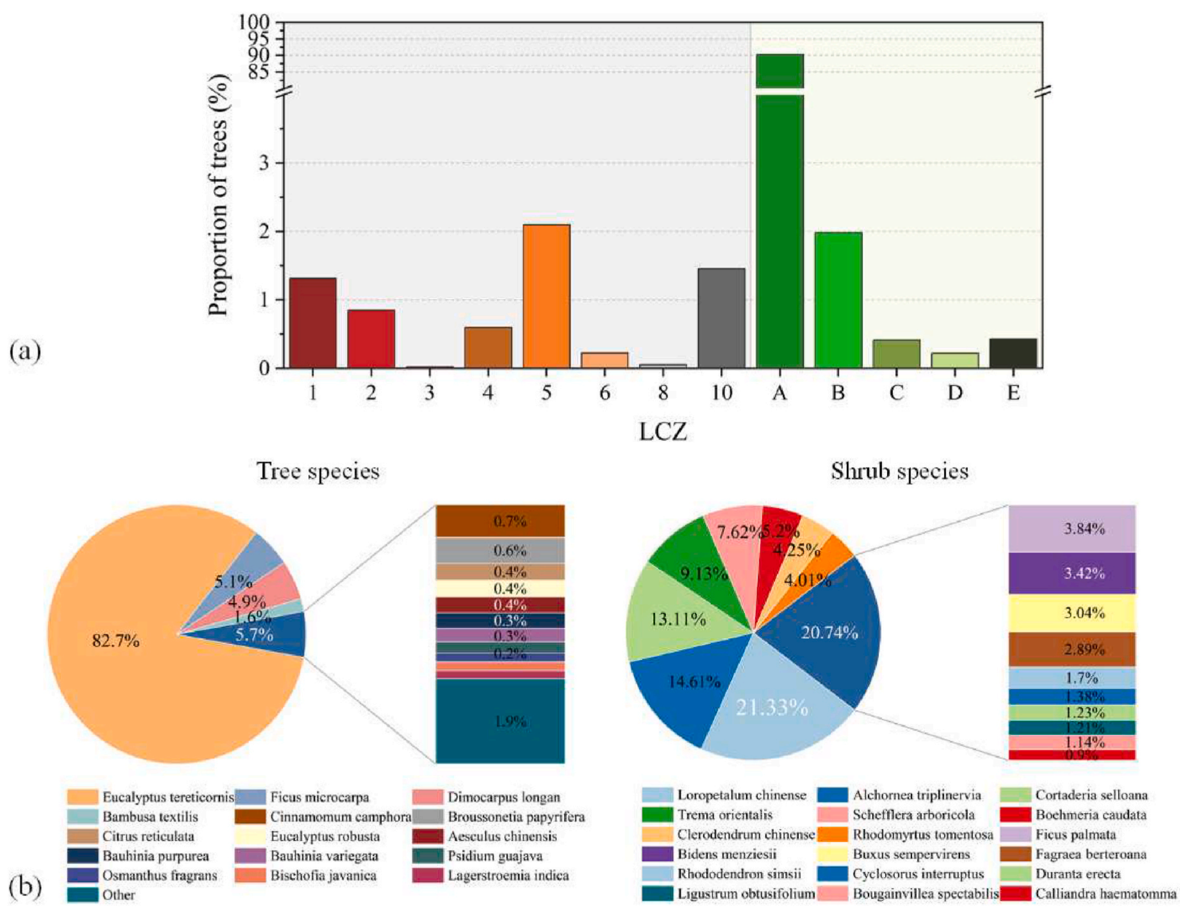

Fig. 4. The proportions and species of trees and shrubs in LCZs (a. the proportions of trees in each LCZ; b. the proportions of tree and shrub species in Guangzhou).

and shrub removal were conducted.

3.3.1.1. Vegetation composition in Guangzhou. Fig. 4 shows the proportions and species of trees and shrubs in each LCZ in 2019. LCZ A accounted for 53.48% of the total area of the city, and *Eucalyptus robusta Smith* (82.7%) was the dominant species. Fig. 4(a) shows that the proportion of trees in the open building area was 0.7% higher than that in the dense building area. The proportion of trees in LCZ 5 accounted for 2.1%, whereas LCZ 3 had the lowest proportion of 0.03%. Fig. 4(b) shows the proportion of each tree and shrub species, from which it was concluded that three tree species, *Ficus microcarpa*, *Dimocarpus longan*, and *Bambusa textilis*, were the dominant species in the area except for the dense forest, with percentages of 5.1%, 4.9%, and 1.6%, respectively, and the total trees of these three species exceeded half in the built type. In terms of shrubs, *Loropetalum chinense* had the highest percentage of 21.3%, followed by *Alchornea triplinervia* (14.6%) and *Cortaderia selloana* (13.1%). Detailed data of species are listed in the Supporting Information (Tables S4 and S5).

3.3.1.2. Air pollution removal by current vegetation. Table 3 shows the total amount of air pollutants removed by trees and shrubs in each LCZ in Guangzhou. It was found that the air pollutants were mainly removed by trees in most LCZs. Compared with other LCZs, the trees in LCZ A had an absolute advantage, accounting for 77% of the total removal by all trees. The annual removal amount of LCZ A reached 56,591 tons, which was more than 1000 times higher than that of the trees in LCZ 3 (50 tons), which had the least amount of pollutants removed. For built types, such as LCZs 1, 2, 5, and 10, trees effectively removed pollutants, although the air quality was rather poor. The overall pollutant removal by shrubs was lower than that of the trees. Nonetheless, the annual removal of shrubs reached 1314 tons in LCZ 1, which was half that of trees. The removal of shrubs even exceeded that of trees in LCZ 4.

The removal of various air pollutants by vegetation in Guangzhou was analyzed and compared, as shown in Fig. 5. Among others, the annual removal of O_3 was the largest at 40,046 tons. In addition to dry deposition, BVOC emissions from vegetation can synergistically promote the absorption of O_3 by leaves (Li et al., 2018). The second most-removed pollutant was NO_2, which was approximately half of that of O_3 (40,046 tons per year), followed by $PM_{2.5}$ (7278 tons per year), which was only 1/5 of that of O_3. The annual removals of SO_2 and CO were the lowest, with values of 5033 and 2674 tons, respectively. In addition, the regional differences were relatively large, especially the range of $PM_{2.5}$, which reached 15,182 tons, exceeding its annual average. A plausible reason is that $PM_{2.5}$ was affected by pollution sources and was greatly affected by precipitation because it was mainly removed by wet deposition.

Table 3
Total pollutants removed by trees and shrubs and the gross carbon sequestration of all trees in 2019.

LCZs	Pollutant Removal (tons)		
	Total	Trees	Shrubs
1: Compact high-rise	2800.803	2212.993	1314.240
2: Compact mid-rise	2040.418	1889.078	192.674
3: Compact low-rise	52.759	49.327	3.651
4: Open high-rise	454.089	315.009	333.993
5: Open mid-rise	4978.814	4620.100	440.957
6: Open low-rise	324.440	300.472	30.373
8: Large low-rise	104.640	95.040	14.959
10: Heavy industry	3293.930	3146.807	42.606
A: Dense trees	59430.397	56590.527	1280.785
B: Scattered trees	2248.853	2126.512	89.560
C: Bush scrub	682.659	257.475	1098.975
D: Low plants	713.493	679.107	16.182
E: Rock paved	1355.614	1279.793	59.714
All	78480.909	73562.240	4918.669

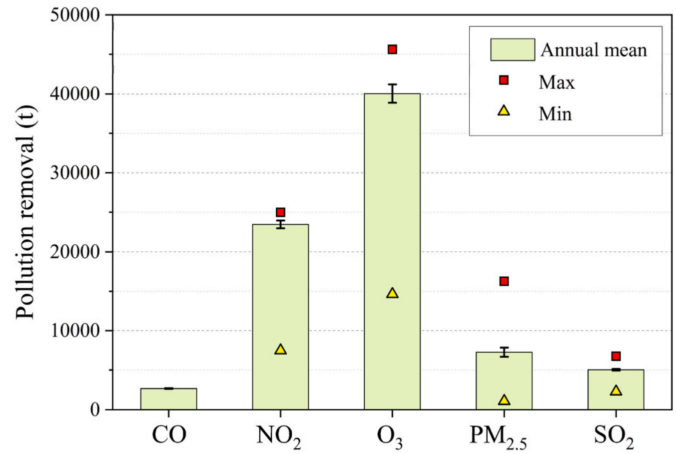

Fig. 5. Maximum, minimum, and annual average removal amount of every pollutant (CO, NO_2, O_3, $PM_{2.5}$, SO_2).

3.3.2. Simulation of adding various trees

3.3.2.1. Air pollution removal of adding street trees. The various and total pollutant removals in each scenario are shown in Fig. 6. In general, adding street trees could increase the total removal with a variation of up to 2%. Compared with the scenarios of adding street trees only in the urban expansion area (T_3, T_4, and T_5), adding trees to the whole built-up area (T_1, T_2) was more effective in removing the total air pollutants, especially T_1, which removed 93.71 tons more air pollutants each year than T_5. Under the T_1, T_2, and T_3 scenarios, the air pollution removal increased by 1.32%, 3.06%, and 0.23%, respectively; the total removal of the T_4 and T_5 scenarios increased by 0.59% and 1.19%, respectively. The larger the coverage of street trees was, the more air pollutants were removed. This result was in accordance with many previous studies in which street trees as roadside vegetation barriers effectively reduced the concentration of air pollutants, especially particulate matter. In addition, the removal was positively correlated with the leaf area index (LAI) and canopy density to a certain extent (Chen et al., 2021; Kończak et al., 2021; Li et al., 2016; Ottosen and Kumar, 2020; Ozdemir, 2019; Wang et al., 2020). In recent years, some researchers have reported that the presence of street trees makes air pollution more serious because vegetation reduces urban aerodynamic effects and decreases air ventilation and eddies, which are not conducive to pollutant dispersion (Chen et al., 2016; Moonen et al., 2013; Morakinyo and Lam, 2016; Xue and Li, 2017). Lin et al. (2020) pointed out that on a larger spatial scale, the deposition of pollutants by vegetation was mainly considered compared with the impact on pollutant diffusion.

The individual removed amounts of CO, NO_2, O_3, $PM_{2.5}$, and SO_2 under each scenario are shown in Fig. 6(a–e). The layout and coverage area of adding street trees affected the amount of removal. The T2 scenario showed the best performance in the removal of all types of pollutants. Specifically, the removal of CO and SO_2 increased by 3.90% and 3.00%, respectively, NO_2 and O_3 showed the same increase of 2.90%, and $PM_{2.5}$ had the smallest increase of 1.79%. Compared with the two scenarios with an overall increase of 5% in built-up area (T_1) and an increase of 20% in the urban expansion area (T_5), the removed amounts of CO, NO_2, O_3, and SO_2 were higher in T_1 than in T_5; however, the removed amount of $PM_{2.5}$was the opposite. This finding may be related to the appropriate canopy density. Wang et al. (2020) pointed out that the greatest reduction of $PM_{2.5}$ occurred at canopy densities ranging from 24% to 36%, and an excessive canopy density led to air quality deterioration. Jin et al. (2014) also showed that regular pruning of street trees was beneficial for air quality optimization. The increase in pollutant removal in T_3 and T_4 was not obvious (less than 0.8%), and the improved efficiency was low.

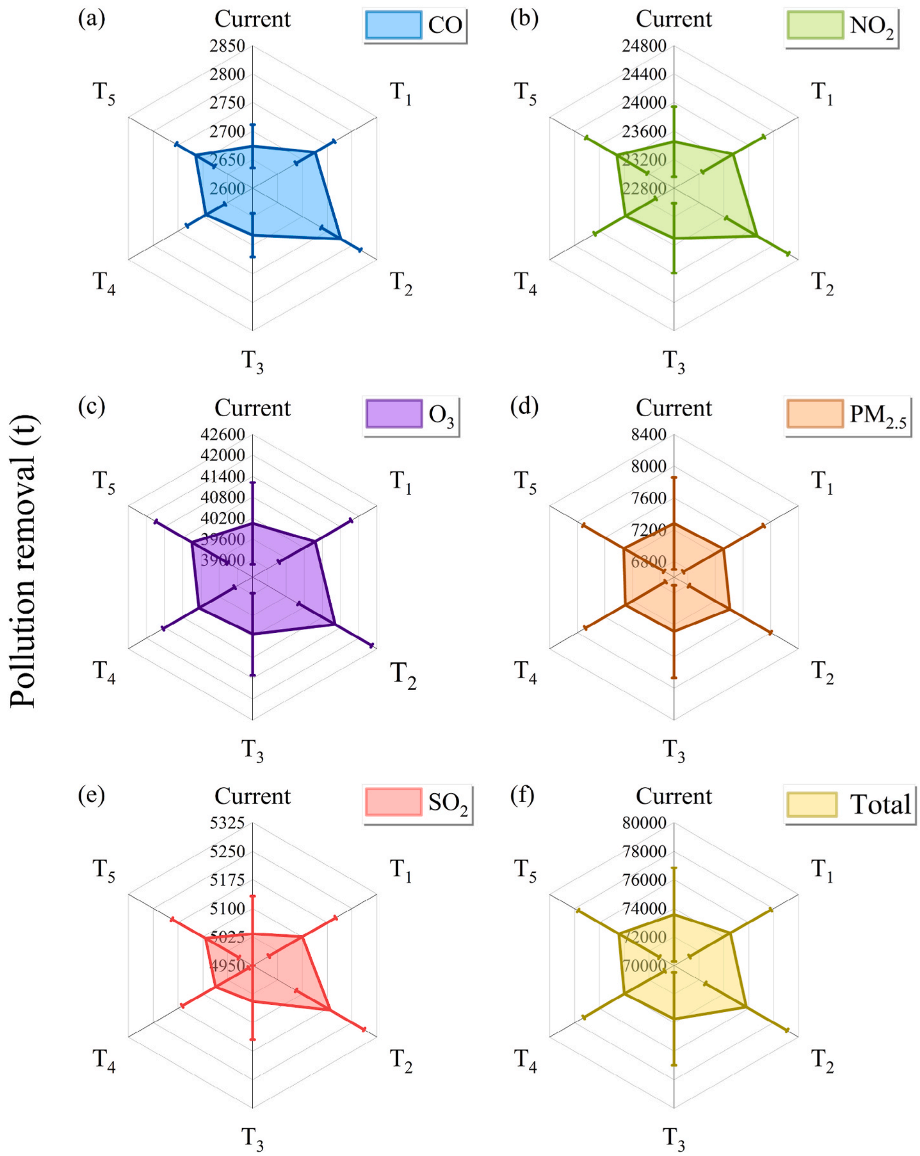

Fig. 6. Annual removal of various pollutants and total pollution under different street trees scenarios (a-e. the amount of CO, NO_2, O_3, $PM_{2.5}$ and SO_2 removed by street trees (*Ficus microcarpa*) under different scenarios; f. total amount of air pollutants removed by street trees under different scenarios).

3.3.2.2. Air pollution removal of adding city parks. Fig. 7 shows the total amount of each pollutant removed (T_a–T_e) under different scenarios in which city park trees were added. UGI types did not affect the order of the total amount of removed pollutants among different scenarios but changed the total amount that was removed. Compared with the current condition, the largest increment in annual total removals was the T_b scenario, with an increase of 2247.55 tons, followed by the T_a, T_e, and T_d scenarios, with increases of 970.09, 871.98, and 423.59 tons, respectively. In terms of the removal of various pollutants, the removal capacity of city park trees under different scenarios was the same as that of the street trees. The pollutants removed, ranked from the most to the least, were O_3, NO_2, $PM_{2.5}$, SO_2, and CO. Although the removal amount of each pollutant varied with the changes in UGIs, the overall removal achieved by adding roadside green space and city park green space was very similar, with a difference of less than 0.02%. Therefore, the comparison of each scenario and between scenarios was also the same.

3.3.2.3. Comparison between adding two types of UGIs. With the same proportion and distribution, the total pollution removal and the amount of each type of pollutant differed but were somewhat very rare under different UGIs. The differences between the two types of UGIs were obtained by subtracting the pollutant removed by street trees from that removed by park trees, as shown in Table 4. In terms of total air pollutant removal, street trees performed better than city park trees under most scenarios, except for one with minimum adding proportion in the urban expansion area (T_3/T_c). This finding indicates that street trees are more effective for air quality improvement when applied on a larger scale with a more addable area, while applying city park trees is an alternative at a local scale with limited area.

For both roadside green space and city park green space, more pollutants were removed as vegetation coverage increased. If only the improvement effect of air quality was considered, the overall increase of 10% vegetation coverage was the most effective. However, according to previous studies in this region and our research experience, it is difficult to achieve the overall increase of 10% greenery coverage in the entire area, because there are not enough available spaces (Li et al., 2020). In addition, large-scale and high-proportion greening is more costly in terms of time, finance, and manpower, which is difficult to achieve. Therefore, on the premise of fully analyzing the current situation and objective condition, T_1/T_a and T_5/T_e were more relatively feasible and

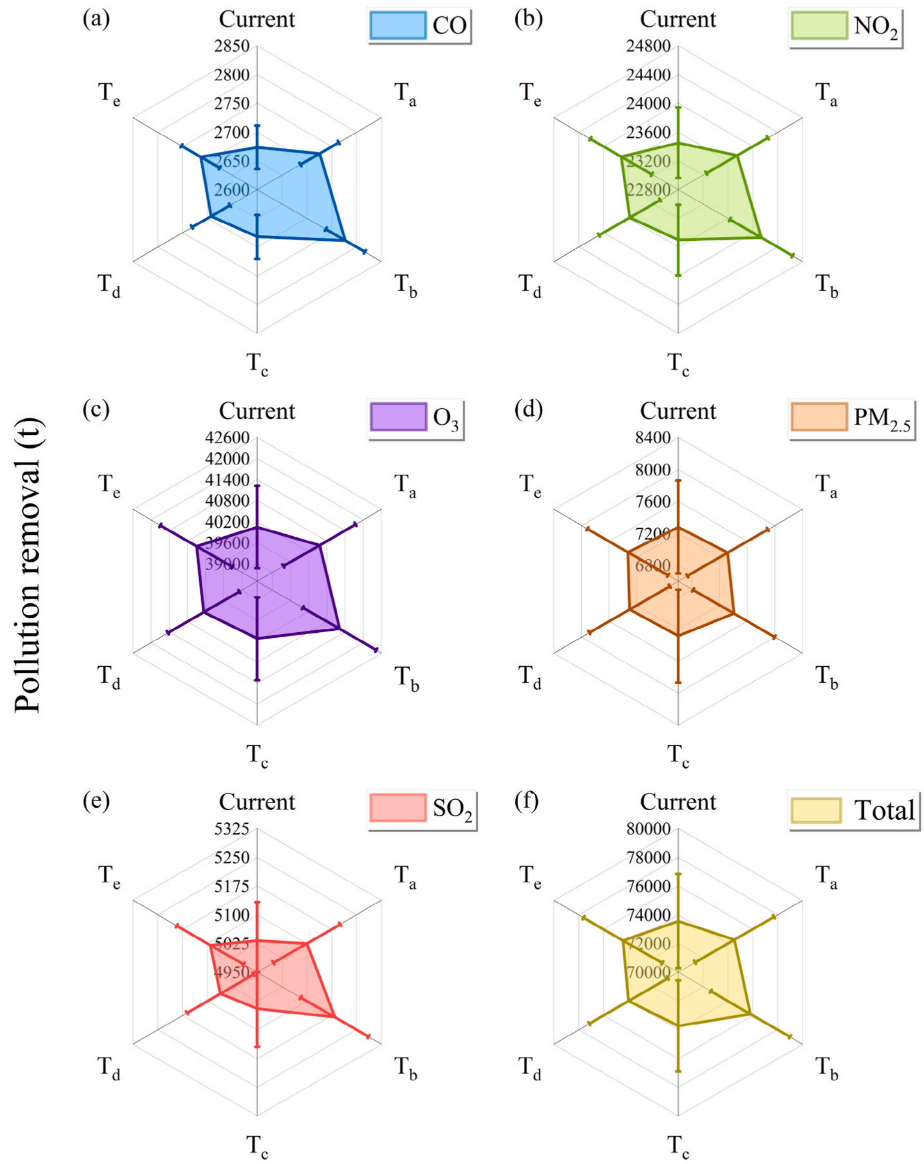

Fig. 7. Annual removal of various pollutants and total pollution under different city park trees scenarios (a-e. the amount of CO, NO_2, O_3, $PM_{2.5}$, and SO_2 removed by city park trees (*Mangifera indica*) under different adding city park trees scenarios, respectively; f. total amount of air pollutants removed by city park trees under different scenarios).

Table 4
The differences between adding street trees and city park trees (The value was obtained by subtracting pollutants removal of street trees from that of park trees).

		T_a-T_1	T_b-T_2	T_c-T_3	T_d-T_4	T_e-T_5
Total removal (tons/yr)		−2.62	−3.29	1.2	−9.37	−7.02
Removal of each pollutant (tons/yr)	CO	0	0	0	−0.92	−1.03
	NO_2	−0.75	−0.95	0.34	−3.07	−2.43
	O_3	−1.26	−1.59	0.58	−5.32	−4.29
	$PM_{2.5}$	−0.45	−0.57	0.21	0.68	1.36
	SO_2	−0.15	−0.18	0.07	−0.74	−0.64

implementable compared with other scenarios. Comparing the two scenarios of an overall increase of 5% in the built-up areas (T_1/T_a) and an increase of 20% in the urban expansion areas (T_5/T_e), the former performed slightly better than the latter in terms of removing most pollutants, but the removal amounts were very similar. The latter even performed better than the former in terms of $PM_{2.5}$ removal. We have fully analyzed the research status and objective factors, T_1/T_a and T_5/T_e were more relatively feasible and implementable compared with other scenarios.

To select the optimal tree scenario with the greatest improvement in air quality in Guangzhou, it was necessary to find the most appropriate UGI type and the optimal greening design for each LCZ type. As mentioned above, T_1/T_a and T_5/T_e had similar effects on air pollution and high applicability. Therefore, the total removed air pollutants in each LCZ for the two UGI types are summarized in Table 5.

Adding city park trees performed better for most LCZs, except for LCZ 6, where the optimal greening design was a 20% increase in street trees in the urban expansion area. Since the greening design was not carried out in land cover types (LCZ A-D), the changes in pollution removal were caused by variations in the LAI. Among the built-up types (LCZs 1–10), LCZ 1, LCZ 3, and LCZ 10 need to add 5% of city park trees to the whole built-up area due to the large pollutant emissions and poor diffusion conditions. For LCZ 2, LCZ 4, LCZ 5, LCZ 8, and LCZ E, the air pollutants were relatively dispersed, and diffusion conditions and tree

Table 5
The annual total pollution removal in each LCZ of the two types of UGIs.

LCZs	Street trees		City park trees	
	T_1 (tons)	T_5 (tons)	T_a (tons)	T_e (tons)
1: Compact high-rise	2360.69	2325.21	2364.81	2327.42
2: Compact mid-rise	1973.04	1985.86	1975.07	1987.78
3: Compact low-rise	51.99	50.21	52.05	50.21
4: Open high-rise	343.01	356.64	343.75	357.67
5: Open mid-rise	4746.33	4819.22	4732.23	4822.84
6: Open low-rise	306.09	317.67	306.20	317.58
8: Large low-rise	98.81	100.67	98.90	100.79
10: Heavy industry	3238.51	3209.14	3240.52	3209.55
A: Dense trees	57022.95	56864.07	57024.65	56847.71
B: Scattered trees	2142.76	2136.79	2142.83	2136.18
C: Bush scrub	259.44	258.72	259.45	258.64
D: Low plants	684.30	682.39	684.32	682.19
E: Rock paved	1307.03	1334.66	1307.56	1335.65

coverage were relatively good. Hence, increasing the city park trees by 20% in urban expansion areas can effectively improve air quality in these LCZs.

3.3.3. Simulation of adding shrubs

There were five scenarios in which shrubs were added, and the scenarios had different layouts and proportions. The total amount of pollutants removed by shrubs under each scenario is shown in Fig. 8. The results showed that the larger the shrub coverage was, the more pollutants were removed. Compared with the trees, the increase in pollution removed by adding shrubs was larger, and the differences between different scenarios were also larger. Hence, shrub coverage was an important factor influencing the total amount of pollutant removal. The S_2 scenario increased air pollution removal by 30.87%, with a value of 6437.07 tons, whereas the S_3 scenario increased air pollution removal by only 4.08%. The annual amount of pollutants removed in the S_4 scenario increased by 7.50%. The increases in pollution removal in the S_1 and S_5 scenarios were similar, with values of 14.72% (5642.82 tons) and 13.75% (5595.13 tons), respectively.

This study selected the optimal shrub layout and proportion for each LCZ to maximize the removal of pollutants. Similar to the trees, although the overall increase of 10% (S_2) in shrubs removed the most pollutants, the scenario would be difficult to implement. In the shrub scenarios with increases of 5% (S_3) and 10% in the urban expansion areas (S_4), the improvement in air quality was small, and the efficiency was low. The

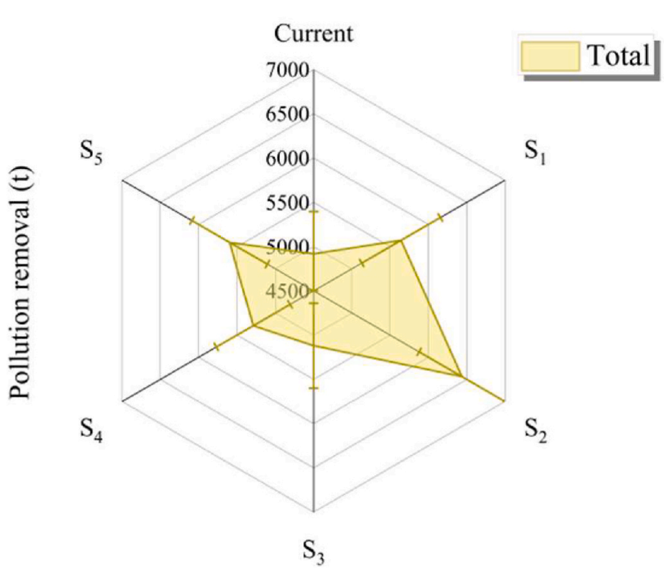

Fig. 8. The annual removal of total air pollution under different shrub scenarios.

overall increase of 5% in the built-up areas (S_1) and the increase of 20% in the urban expansion areas (S_5) showed similar performance in air pollution removal. The total amount of pollutants removed in each LCZ under these two scenarios are summarized in Table 6. For the built types, LCZ 1, LCZ 3, LCZ 4, and LCZ 10 were suitable for adding 5% shrub coverage in the built-up areas, while in LCZ 2, LCZ 5, LCZ 6, LCZ 8, and LCZ E, adding 20% shrub coverage in the urban expansion area achieved better air quality improvement.

3.3.4. Final optimal design

After obtaining the optimal tree and shrub scenarios, we integrated the two to obtain the final optimal design for each LCZ in Guangzhou.

1) For LCZ 1, LCZ 3, and LCZ 10 with large air pollution emissions and less vegetation, the overall 5% increase in the built-up areas was selected for both trees and shrubs, and city park trees were adopted as the greening UGI.
2) Although LCZ 2, LCZ 5, LCZ 6, LCZ 8, and LCZ E had large pollutant emissions, there were certain vegetation coverage and diffusion conditions. Therefore, the vegetation was added at a local scale, that is, adding 20% vegetation in urban expansion areas. The types of trees added were all city park trees except LCZ 6, which was street trees.
3) There were a large number of trees in LCZ 4; hence, we added city park trees by 20% in the urban expansion area to obtain the best air quality improvement within the limited area. Moreover, 5% of shrubs were added to the whole built-up area to maximize the total pollutant removal amount.

In addition, the land cover types (except LCZ E) were not changed. The distribution of the optimal UGI design in Guangzhou city is shown in Fig. 9.

3.4. Limitations of the research

This study has some considerations and limitations. First, the complex urban building morphology of Guangzhou may involve multiple LCZ types in a small area. Therefore, the accuracy of the surface division of built-up areas based on Landsat images is limited. Future studies can finely classify or construct a high-precision classification system based on specific urban morphological parameters in complex built-up areas to improve the LCZ classification of Guangzhou city. Second, i-Tree Eco as a status quo-based efficiency model is seldom validated. Future research should carry out the validation by comparing the simulation results with measurements to ensure the accuracy and reliability of the research findings. Third, the number of meteorological stations is small, and the coverage area of the model database is limited. There is only one meteorological station in Baiyun District in Guangzhou, which makes the simulation results in areas far from the weather stations biased to a certain extent. Fourth, only two common UGIs (i.e., roadside green

Table 6
The annual total removal of pollution in each LCZ type under the two scenarios.

LCZ Types	S_1 (tons)	S_5 (tons)
1: Compact high-rise	1593.57	1484.41
2: Compact mid-rise	323.03	370.73
3: Compact low-rise	6.11	5.02
4: Open high-rise	379.40	356.96
5: Open mid-rise	564.54	610.98
6: Open low-rise	35.27	42.69
8: Large low-rise	19.71	22.11
10: Heavy industry	163.11	161.91
A: Dense trees	1273.41	1251.52
B: Scattered trees	89.04	87.51
C: Bush scrub	1092.64	1073.87
D: Low plants	16.09	15.81
E: Rock paved	86.88	111.60

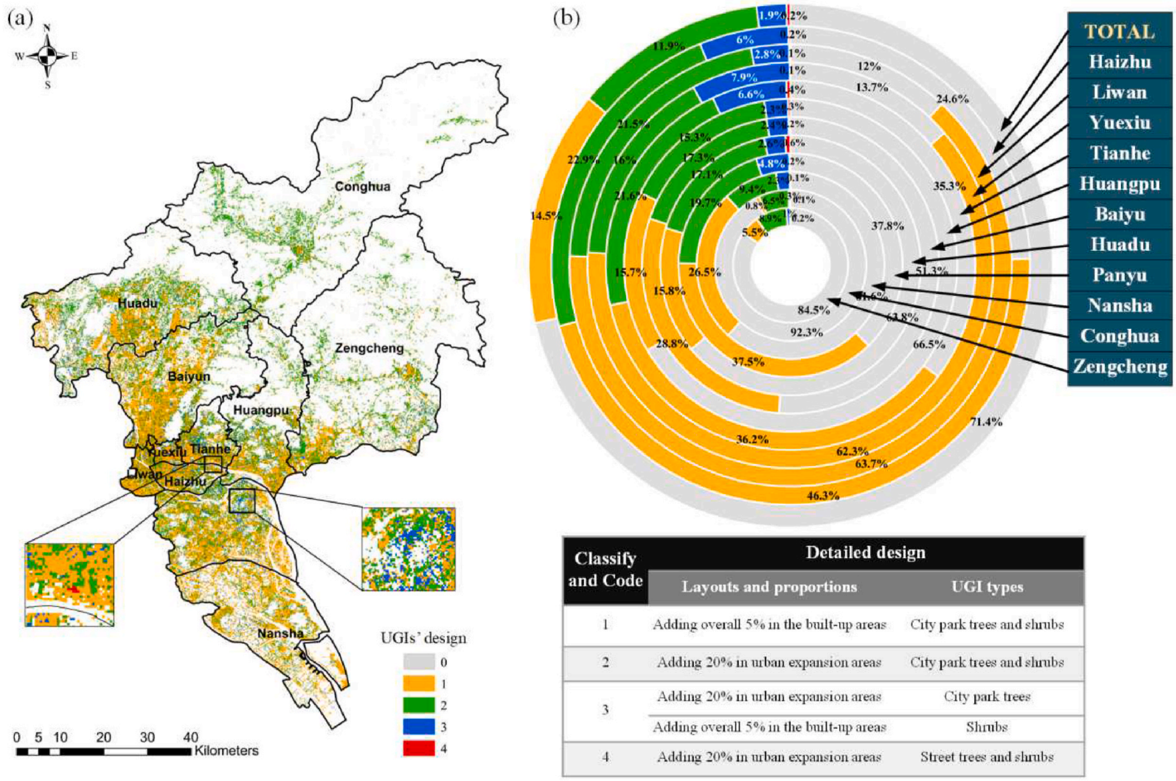

Classify and Code	Detailed design: Layouts and proportions	UGI types
1	Adding overall 5% in the built-up areas	City park trees and shrubs
2	Adding 20% in urban expansion areas	City park trees and shrubs
3	Adding 20% in urban expansion areas	City park trees
	Adding overall 5% in the built-up areas	Shrubs
4	Adding 20% in urban expansion areas	Street trees and shrubs

Fig. 9. The distribution of the optimal UGIs design in Guangzhou city (a. the UGIs' design distribution in Guangzhou; b. the proportion of different UGI's design in each district of Guangzhou.).

space and city park green space) and the two elements that comprise them (i.e., trees and shrubs) were explored in this study, and more elements and some small UGIs, such as green roofs and green walls, should be included in future studies. Finally, i-Tree Eco requires a large amount of vegetation data for simulation and quantification. However, the wide variety of vegetation in Guangzhou and the large vegetation area in some areas make it difficult to collect data. In future research, multidisciplinary vegetation surveys can be carried out jointly, such as botany and surveying and mapping, and comprehensive and accurate vegetation data can be obtained under the leadership of professional institutions to obtain a more complete evaluation of UGIs in Guangzhou.

Despite these limitations, this study analyzed the impact of urban form changes on air quality due to urbanization, expanded the research scope of LCZ analysis, and explored the possibilities of this method in fields other than urban heat island research. In addition, the i-Tree Eco model was used for the first time in China to simulate, quantify, and optimize the scenario of UGIs in different urban forms. Compared with the existing research that studies only the current situation and benefits of UGIs in a local region, this study has stronger guiding significance for urban design and planning.

4. Conclusion

Finding the most effective UGI strategies for air quality improvement at the urban scale using multiple scenario simulations is essential for green, healthy, and sustainable urban planning and design. Integrating LCZs with the i-Tree Eco simulation tool can be used to quantitatively analyze the structure and pollutant removal benefits of existing UGIs in Guangzhou and further explore sustainable UGI strategies to identify the best types and densities of UGIs in different areas to improve air quality in Guangzhou. The practical method developed in this research provides helpful guidelines for urban green development.

From 2013 to 2019, the built-type LCZ gradually replaced the land cover-type LCZ in Guangzhou, indicating that the city was expanding and the urbanization process was rapid. There were two main development trends: one was the continuous increase in dense buildings (LCZs 1–3) to adapt to the current situation of rapid population growth and meet the requirements of high-speed economic development; another was the dramatic increase in open buildings (LCZs 4–6) to provide a more comfortable and beautiful living environment for people. High-intensity urban development harms urban air quality. Taking $PM_{2.5}$ as the representative, the concentration of built-type LCZs was higher than that of land cover type LCZs. To some extent, it also indicated that in addition to land-use types, urban form has a great impact on air quality.

According to the i-Tree Eco model, we found that the larger the LAI increased, the more total pollution and the more of each type of pollutant were removed for both trees and shrubs. For trees, city park trees were more advantageous for local scale areas, while street trees performed better in the large-scale regions. In terms of the proportion added, adding an overall of 5% vegetation in the built-up area was similar to adding 20% in the urban expansion areas, and both scenarios could be implemented more strongly.

To maximize air quality improvement in Guangzhou, the optimal layouts and proportions of trees and shrubs in the UGI were selected for each LCZ. For LCZ 2, LCZ 5, LCZ 8, and LCZ E, the air quality could be improved best by adding 20% city park trees and shrubs to the urban expansion area. Adding 5% city park trees and shrubs to the whole built-up area in LCZ 1, LCZ 3, and LCZ 10 removed the most air pollutants. The optimal design for LCZ 4 was to add 20% city park trees in the urban expansion area and 5% shrubs in the whole built-up area. For LCZ 6, the optimal UGI design was to add 20% street trees and shrubs in the urban expansion area.

In conclusion, it is suggested that decision-makers and urban planners should consider both the impact of urban form and building layout on air pollution and the improvement effect of different types of UGIs on air quality. Under the premise of ensuring enforceability, the optimal design with the highest pollution removal should be selected for different urban forms and building layouts. The results of this study have strong guiding significance for urban design and planning.

CRediT authorship contribution statement

Yibo Yao: Conceptualization, Methodology, Data curation, Writing – original draft. **Yafei Wang:** Visualization. **Zhuobiao Ni:** Writing – review & editing. **Shaoqing Chen:** Project administration. **Beicheng Xia:** Project administration.

Declaration of competing interest

The authors declare that they have no known competing financial interests or personal relationships that could have appeared to influence the work reported in this paper.

Data availability

Data will be made available on request.

Acknowledgments

This research was financially supported by the National Key R&D Program of China (2016YFC0502803), Guangdong Provincial Science and Technology Project (2019A1515011580, 2022A1515011929, 2021B1212040008).

Appendix A. Supplementary data

Supplementary data to this article can be found online at https://doi.org/10.1016/j.jclepro.2022.133372.

References

Aslan, A., Altinoz, B., Ozsolak, B., 2021. The link between urbanization and air pollution in Turkey: evidence from dynamic autoregressive distributed lag simulations. Environ. Sci. Pollut. Control Ser. 28 (37), 52370–52380.
Auer, A.H., 1978. Correlation of land use and cover with meteorological anomalies. J. Appl. Meteorol. 17 (5), 636–643.
Baetjer, A.J., 1950. Chronic exposures to air pollutants and acute infectious respiratory diseases. Arch. Ind. Hyg. Occup. Med. 2 (4), 400–406.
Benedict, M.A., McMahon, E.T., 2002. Green infrastructure: smart conservation for the 21st century. Renew. Resour. J. 20 (3), 12–17.
Boningari, T., Smirniotis, P.G., 2016. Impact of nitrogen oxides on the environment and human health: Mn-based materials for the NOx abatement. Current Opinion in Chemical Engineering 13, 133–141.
Bottalico, F., Chirici, G., Giannetti, F., De Marco, A., Nocentini, S., Paoletti, E., Salbitano, F., Sanesi, G., Serenelli, C., Travaglini, D., 2016. Air pollution removal by green infrastructures and urban forests in the city of Florence. Agriculture and agricultural science procedia 8, 243–251.
Brousse, O., Martilli, A., Foley, M., Mills, G., Bechtel, B., 2016. WUDAPT, an efficient land use producing data tool for mesoscale models? Integration of urban LCZ in WRF over Madrid. Urban Clim. 17, 116–134.
Cai, M., Ren, C., Xu, Y., Dai, W., Wang, X.M., 2016. Local climate zone study for sustainable megacities development by using improved WUDAPT methodology–a case study in Guangzhou. Procedia Environmental Sciences 36, 82–89.
Calfapietra, C., Fares, S., Manes, F., Morani, A., Sgrigna, G., Loreto, F., 2013. Role of Biogenic Volatile Organic Compounds (BVOC) emitted by urban trees on ozone concentration in cities: a review. Environ. Pollut. 183, 71–80.
Chen, G., Xie, J., Li, W., Li, X., Chung, L., Ren, C., Liu, X., 2021. Future "local climate zone" spatial change simulation in Greater Bay Area under the shared socioeconomic pathways and ecological control line. Build. Environ. 203, 13.
Chen, L., Liu, C., Zou, R., Yang, M., Zhang, Z., 2016. Experimental examination of effectiveness of vegetation as bio-filter of particulate matters in the urban environment. Environ. Pollut. 208, 198–208.
Chen, X., Wang, X., Wu, X., Guo, J., Zhou, Z., 2021. Influence of Roadside Vegetation Barriers on Air Quality inside Urban Street Canyons. Urban Forestry & Urban Greening, 127219.
Chen, X., Xu, Y., Yang, J., Wu, Z., Zhu, H., 2020. Remote sensing of urban thermal environments within local climate zones: a case study of two high-density subtropical Chinese cities. Urban Clim. 31, 10.
Chen, X., Yang, J., Ren, C., Jeong, S., Shi, Y., 2021. Standardizing thermal contrast among local climate zones at a continental scale: implications for cool neighborhoods. Build. Environ. 197, 10.
Ching, J., Aliaga, D., Mills, G., Masson, V., See, L., Neophytou, M., Middel, A., Baklanov, A., Ren, C., Ng, E., Fung, J., Wong, M., Huang, Y., Martilli, A., Brousse, O., Stewart, L., Zhang, X.W., Shehata, A., Miao, S.G., Wang, X.M., Wang, W.W., Yamagata, Y., Duarte, D., Li, Y.G., Feddema, J., Bechtel, B., Hidalgo, J., Roustan, Y., Kim, Y., Simon, H., Kropp, T., Bruse, M., Lindberg, F., Grimmond, S., Demuzure, M., Chen, F., Li, C., Gonzales-Cruz, J., Bornstein, B., He, Q.D., Tzu, P., Hanna, A., Erell, E., Tapper, N., Mall, R.K., Niyogi, D., 2019. Pathway using WUDAPT's Digital Synthetic City tool towards generating urban canopy parameters for multi-scale urban atmospheric modeling. Urban Clim. 28, 23.
Ching, J., Mills, G., Bechtel, B., See, L., Feddema, J., Wang, X., Ren, C., Brousse, O., Martilli, A., Neophytou, M., 2018. WUDAPT: an urban weather, climate, and environmental modeling infrastructure for the anthropocene. Bull. Am. Meteorol. Soc. 99 (9), 1907–1924.
Chu, Z., Bian, C., Yang, J., 2021. Joint prevention and control mechanism for air pollution regulations in China: a policy simulation approach with evolutionary game. Environ. Impact Assess. Rev. 91.
Demuzere, M., Bechtel, B., Mills, G., 2019. Global transferability of local climate zone models. Urban Clim. 27, 46–63.
Eldesoky, A., Gil, J., Pont, M., 2021. The suitability of the urban local climate zone classification scheme for surface temperature studies in distinct macroclimate regions. Urban Clim. 37, 22.
Ellefsen, R., 1991. Mapping and measuring buildings in the canopy boundary layer in ten U.S. cities. Energy Build. 16, 1025–1049.
Estacio, I., Babaan, J., Pecson, N., Blanco, A., Escoto, J., Alcantara, C., 2019. GIS-BASED mapping of local climate zones using fuzzy logic and cellular automata. In: International Archives of the Photogrammetry. Remote Sensing & Spatial Information Sciences.
Fan, J., 2019. Study on the Quantity Change and Utilization of Agricultural Land in Baiyun District of Guangzhou City. Zhongkai University of Agriculture and Engineering.
Foster, J., Lowe, A., Winkelman, S., 2011. The value of green infrastructure for urban climate adaptation. Center for Clean Air Policy 750 (1), 1–52.
Hidalgo, J., Dumas, G., Masson, V., Petit, G., Bechtel, B., Bocher, E., Foley, M., Schoetter, R., Mills, G., 2019. Comparison between local climate zones maps derived from administrative datasets and satellite observations. Urban Clim. 27, 64–89.
Holec, J., Feranec, J., Stastny, P., Szatmari, D., Kopecka, M., Garaj, M., 2020. Evolution and assessment of urban heat island between the years 1998 and 2016: case study of the cities Bratislava and Trnava in western Slovakia. Theor. Appl. Climatol. 141 (3–4), 979–997.
Huang, D., He, B., Wei, L., Sun, L., Li, Y., Yan, Z., Wang, X., Chen, Y., Li, Q., Feng, S., 2021. Impact of land cover on air pollution at different spatial scales in the vicinity of metropolitan areas. Ecol. Indicat. 132.
Huang, L., 2017. Study of City Village Reconstruction in Guang Zhou ——A Case Study of Yagang Village. South China University of Technology.
Huang, Q., Xu, C., Jiang, W., Yue, W., Rong, Q., Gu, Z., Su, M., 2021. Urban compactness and patch complexity influence PM2. 5 concentrations in contrasting ways: evidence from the Guangdong-Hong Kong-Macao Greater Bay Area of China. Ecol. Indicat. 133, 108407.
i-Tree Eco User's Manual, 2020. https://www.itreetools.org/support/resources-overview/i-tree-manuals-workbooks. (Accessed 20 August, 2020).
Jayasooriya, V., Ng, A., Muthukumaran, S., Perera, B., 2017. Green infrastructure practices for improvement of urban air quality. Urban For. Urban Green. 21, 34–47.
Jiang, W., Gao, W., Gao, X., Ma, M., Zhou, M., Du, K., Ma, X., 2021. Spatio-temporal heterogeneity of air pollution and its key influencing factors in the Yellow River Economic Belt of China from 2014 to 2019. J. Environ. Manag. 296, 12.
Jin, S., Guo, J., Wheeler, S., Kan, L., Che, S., 2014. Evaluation of impacts of trees on PM2. 5 dispersion in urban streets. Atmos. Environ. 99, 277–287.
Khamchiangta, D., Dhakal, S., 2021. Future urban expansion and local climate zone changes in relation to land surface temperature: case of Bangkok Metropolitan Administration, Thailand. Urban Clim. 37, 16.
Kim, K.-H., Kabir, E., Kabir, S., 2015. A review on the human health impact of airborne particulate matter. Environ. Int. 74, 136–143.
Kończak, B., Cempa, M., Deska, M., 2021. Assessment of the ability of roadside vegetation to remove particulate matter from the urban air. Environ. Pollut. 268, 115465.
La, Y., Bagan, H., Yamagata, Y., 2020. Urban land cover mapping under the Local Climate Zone scheme using Sentinel-2 and PALSAR-2 data. Urban Clim. 33, 14.
Lau, K.K.-L., Chung, S.C., Ren, C., 2019. Outdoor thermal comfort in different urban settings of sub-tropical high-density cities: an approach of adopting local climate zone (LCZ) classification. Build. Environ. 154, 227–238.
Lei, Y., Davies, G.M., Jin, H., Tian, G., Kim, G., 2021. Scale-dependent effects of urban greenspace on particulate matter air pollution. Urban For. Urban Green. 61, 9.
Li, J., Wang, Y., Ni, Z., Chen, S., Xia, B., 2020. An integrated strategy to improve the microclimate regulation of green-blue-grey infrastructures in specific urban forms. J. Clean. Prod. 271, 122555.
Li, Q., Gabay, M., Rubin, Y., Fredj, E., Tas, E., 2018. Measurement-based investigation of ozone deposition to vegetation under the effects of coastal and photochemical air pollution in the Eastern Mediterranean. Sci. Total Environ. 645, 1579–1597.
Li, X.-B., Lu, Q.-C., Lu, S.-J., He, H.-D., Peng, Z.-R., Gao, Y., Wang, Z.-Y., 2016. The impacts of roadside vegetation barriers on the dispersion of gaseous traffic pollution in urban street canyons. Urban For. Urban Green. 17, 80–91.

Li, Y., Wang, W., Chang, M., Wang, X., 2021. Impacts of urbanization on extreme precipitation in the Guangdong-Hong Kong-Macau greater Bay area. Urban Clim. 38, 15.
Liang, L., Wang, Z., Li, J., 2019a. The effect of urbanization on environmental pollution in rapidly developing urban agglomerations. J. Clean. Prod. 237.
Liang, L., Wang, Z., Li, J., 2019b. The effect of urbanization on environmental pollution in rapidly developing urban agglomerations. J. Clean. Prod. 237, 117649.
Liang, Z., Huang, J., Wang, Y., Wei, F., Wu, S., Jiang, H., Zhang, X., Li, S., 2021a. The mediating effect of air pollution in the impacts of urban form on nighttime urban heat island intensity. Sustain. Cities Soc. 74.
Liang, Z., Wang, W., Wang, Y., Ma, L., Liang, C., Li, P., Yang, C., Wei, F., Li, S., Zhang, L., 2021b. Urbanization, ambient air pollution, and prevalence of chronic kidney disease: a nationwide cross-sectional study. Environ. Int. 156, 106752.
Lin, G., Fu, J., Jiang, D., Hu, W., Dong, D., Huang, Y., Zhao, M., 2014. Spatio-Temporal variation of PM2.5 concentrations and their relationship with geographic and socioeconomic factors in China. Int. J. Environ. Res. Publ. Health 11 (1), 173–186.
Lin, X., Chamecki, M., Yu, X., 2020. Aerodynamic and deposition effects of street trees on PM2. 5 concentration: from street to neighborhood scale. Build. Environ. 185, 107291.
Liu, Z., Hu, B., Liu, Q., Sun, Y., Wang, Y., 2014. Source apportionment of urban fine particle number concentration during summertime in Beijing. Atmos. Environ. 96, 359–369.
Meng, L., Sun, Y., Zhao, S., 2020. Comparing the spatial and temporal dynamics of urban expansion in Guangzhou and Shenzhen from 1975 to 2015: a case study of pioneer cities in China's rapid urbanization. Land Use Pol. 97, 104753.
Mills, G., Ching, J., See, L., Bechtel, B., 2015. An Introduction to the WUDAPT project. In: Proceedings of the 9th International Conference on Urban Climate, pp. 20–24. Toulouse, France.
Moonen, P., Gromke, C., Dorer, V., 2013. Performance assessment of Large Eddy Simulation (LES) for modeling dispersion in an urban street canyon with tree planting. Atmos. Environ. 75, 66–76.
Morakinyo, T.E., Lam, Y.F., 2016. Study of traffic-related pollutant removal from street canyon with trees: dispersion and deposition perspective. Environ. Sci. Pollut. Control Ser. 23 (21), 21652–21668.
Nowak, D., Riviere, E., Mehdi, L., Weber, C., Selmi, W., 2016. Air Pollution Removal by Trees in Public Green Spaces in Strasbourg City, France. Urban Forestry & Urban Greening.
Nowak, D.J., Walton, J.T., Stevens, J.C., Crane, D.E., Hoehn, R.E., 2008. Effect of plot and sample size on timing and precision of urban forest assessment. Aboriculture & Urban Forestry 34 (6), 386–390.
Oliveira, A., Lopes, A., Niza, S., 2020. Local climate zones in five southern European cities: an improved GIS-based classification method based on Copernicus data. Urban Clim. 33, 25.
Ottosen, T.-B., Kumar, P., 2020. The influence of the vegetation cycle on the mitigation of air pollution by a deciduous roadside hedge. Sustain. Cities Soc. 53, 101919.
Ozdemir, H., 2019. Mitigation impact of roadside trees on fine particle pollution. Sci. Total Environ. 659, 1176–1185.
Quan, J., 2019. Enhanced geographic information system-based mapping of local climate zones in Beijing, China. Sci. China Technol. Sci. 62 (12), 2243–2260.
Ren, Y., Ge, Y., Ma, D., Song, X., Shi, Y., Pan, K., Qu, Z., Guo, P., Han, W., Chang, J., 2017. Enhancing plant diversity and mitigating BVOC emissions of urban green spaces through the introduction of ornamental tree species. Urban For. Urban Green. 27, 305–313.
Riondato, E., Pilla, F., Basu, A.S., Basu, B., 2020. Investigating the effect of trees on urban quality in Dublin by combining air monitoring with i-Tree Eco model. Sustain. Cities Soc. 61, 13.
Santri, I.N., Jiang, C.-B., Chen, Y.-H., Wu, C.-D., Zou, M.-L., Chien, L.-C., Lo, Y.-C., Chao, H.J., 2021. Associations of birth outcomes with air pollution and land use characteristics in the Greater Taipei Area. Sci. Total Environ. 750.
Selmi, W., Weber, C., Rivière, E., Blond, N., Mehdi, L., Nowak, D., 2016. Air pollution removal by trees in public green spaces in Strasbourg city, France. Urban For. Urban Green. 17, 192–201.
Shi, Y., Ren, C., Lau, K.K.-L., Ng, E., 2019. Investigating the influence of urban land use and landscape pattern on PM2. 5 spatial variation using mobile monitoring and WUDAPT. Landsc. Urban Plann. 189, 15–26.
Stewart, I.D., Oke, T.R., 2012. Local climate zones for urban temperature studies. Bull. Am. Meteorol. Soc. 93 (12), 1879–1900.
Tuo, Y., Li, X., Wang, J., 2013. Negative Effects of Beijing's Air Pollution Caused by Urbanization on Residents' Health, 2nd International Conference on Science and Social Research (ICSSR). PEOPLES R CHINA, Beijing, pp. 732–735.
Wang, R., Bai, Y., Alatalo, J.M., Yang, Z., Yang, Z., Yang, W., Guo, G., 2021. Impacts of rapid urbanization on ecosystem services under different scenarios-A case study in Dianchi Lake Basin, China. Ecol. Indicat. 130, 11.
Wang, R., Ren, C., Xu, Y., Lau, K.K.-L., Shi, Y., 2018. Mapping the local climate zones of urban areas by GIS-based and WUDAPT methods: a case study of Hong Kong. Urban Clim. 24, 567–576.
Wang, S., Gao, S., Li, S., Feng, K., 2020. Strategizing the relation between urbanization and air pollution: empirical evidence from global countries. J. Clean. Prod. 243.
Wang, S., Zhou, C., Wang, Z., Feng, K., Hubacek, K., 2017. The characteristics and drivers of fine particulate matter (PM2.5) distribution in China. J. Clean. Prod. 142, 1800–1809.
Wang, X., Teng, M., Huang, C., Zhou, Z., Chen, X., Xiang, Y., 2020. Canopy density effects on particulate matter attenuation coefficients in street canyons during summer in the Wuhan metropolitan area. Atmos. Environ. 240, 117739.
Wang, X., Yan, F., Su, F., 2021. Changes in coastline and coastal reclamation in the three most developed areas of China, 1980–2018. Ocean Coast Manag. 204, 105542.
Wang, Y., Guo, Z., Han, J., 2021. The relationship between urban heat island and air pollutants and them with influencing factors in the Yangtze River Delta, China. Ecol. Indicat. 129, 107976.
Wang, Y., Ni, Z., Hu, M., Chen, S., Xia, B., 2021. A practical approach of urban green infrastructure planning to mitigate urban overheating: a case study of Guangzhou. J. Clean. Prod. 287.
Wu, J., Wang, Y., Qiu, S., Peng, J., 2019. Using the modified i-Tree Eco model to quantify air pollution removal by urban vegetation. Sci. Total Environ. 688, 673–683.
Wu, S., Wang, P., Tong, X., Tian, H., Zhao, Y., Luo, M., 2021. Urbanization-driven increases in summertime compound heat extremes across China. Sci. Total Environ. 799, 11.
Xie, N., Liu, S., 2019. Spatial pattern of urban green spaces and its effects on land use intensification in Guangzhou City. Ecological Science 38 (3), 55–63.
Xu, G., Ren, X., Xiong, K., Li, L., Bi, X., Wu, Q., 2020. Analysis of the driving factors of PM2. 5 concentration in the air: a case study of the Yangtze River Delta, China. Ecol. Indicat. 110, 105889.
Xu, X., Xie, Y., Qi, K., Luo, Z., Wang, X., 2018. Detecting the response of bird communities and biodiversity to habitat loss and fragmentation due to urbanization. Sci. Total Environ. 624, 1561–1576.
Xue, F., Li, X., 2017. The impact of roadside trees on traffic released PM10 in urban street canyon: aerodynamic and deposition effects. Sustain. Cities Soc. 30, 195–204.
Yang, J., Jin, S., Xiao, X., Jin, C., Xia, J.C., Li, X., Wang, S., 2019. Local climate zone ventilation and urban land surface temperatures: towards a performance-based and wind-sensitive planning proposal in megacities. Sustain. Cities Soc. 47, 101487.
Yang, J., Ren, J., Sun, D., Xiao, X., Xia, J., Jin, C., Li, X., 2021. Understanding land surface temperature impact factors based on local climate zones. Sustain. Cities Soc. 69, 10.
Yang, J., Wang, Y., Xiu, C., Xiao, X., Xia, J., Jin, C., 2020. Optimizing local climate zones to mitigate urban heat island effect in human settlements. J. Clean. Prod. 275, 12.
Zhang, G., Yang, R., 2021. Study on Spatio-Temporal Change and Optimization of Spatial Pattern of Guangzhou, 2020/2021 China Urban Planning Annual Conference and 2021 China Urban Planning Academic Season, p. 9. Chengdu, Sichuan, China.
Zhang, H., Zhan, Y., Li, J., Chao, C., Liu, Q., Wang, C., Jia, S., Ma, L., Biswas, P., 2021. Using Kriging incorporated with wind direction to investigate ground-level PM2.5 concentration. Sci. Total Environ. 751, 14.
Zhang, Y., Bash, J.O., Roselle, S.J., Shatas, A., Repinsky, A., Mathur, R., Hogrefe, C., Piziali, J., Jacobs, T., Gilliland, A., 2020. Unexpected air quality impacts from implementation of green infrastructure in urban environments: a Kansas City case study. Sci. Total Environ. 744, 10.
Zhao, X., Zhou, W., Wu, T., Han, L., 2022. The impacts of urban structure on PM2.5 pollution depend on city size and location. Environ. Pollut. 292.
Zhao, Z., Shen, L., Li, L., Wang, H., He, B.-J., 2020. Local climate zone classification scheme can also indicate local-scale urban ventilation performance: an evidence-based study. Atmosphere 11 (8), 776.
Zheng, Y., Ren, C., Xu, Y., Wang, R., Ho, J., Lau, K., Ng, E., 2018. GIS-based mapping of Local Climate Zone in the high-density city of Hong Kong. Urban Clim. 24, 419–448.
Zhou, X., Okaze, T., Ren, C., Cai, M., Ishida, Y., Mochida, A., 2020. Mapping local climate zones for a Japanese large city by an extended workflow of WUDAPT Level 0 method. Urban Clim. 33, 17.
Zhuang, H., 2019. Dynamic change of city Greenland in Guangzhou. Journal of Anhui Agricultural Sciences 47 (16), 138–141.